ISSN No:-2456-2165 https://doi.org/10.38124/ijisrt/26nov1139

Development and Characterization of Ruxolitinib-Loaded Transfersomal Gel: Physicochemical Properties and in Vitro Release

Rahul Dewangan[1]; Dr. Amit Sahu[2]; Arti Solanki[3]; Dr. S. Nayak[4]

[1]Research Scholar, Bansal College of Pharmacy, Bhopal
[2]Professor, Department of Pharmaceutics, Bansal College of Pharmacy, Bhopal
[3]Assistant Professor, Department of Pharmaceutics, Bansal College of Pharmacy, Bhopal
[4]Director, Bansal College of Pharmacy, Bhopal

Publication Date: 2026/11/28

Abstract: Ruxolitinib is effective in conventional topical creams, but alternative vehicles require their own physicochemical and delivery assessment. This study evaluated the formulation rationale, reported characterization and release behavior of ruxolitinib transfersomal gels. The thesis described thin-film hydration with soya phosphatidylcholine, Tween 80 and ethanol, followed by incorporation into Carbopol 940 gels. Fourteen vesicle formulations and three gel variants were documented. Numerical series, instrument images and calculations were examined without treating thesis-labeled illustrative data as independently verified measurements. Reported vesicle sizes ranged from 148.6 to 196.8 nm, with polydispersity indices of 0.198-0.312 and zeta potentials of -26.2 to -17.2 mV. Candidate TF8 had reported entrapment efficiency of 88.64 ± 0.52%. Gel TG2 contained 0.75% Carbopol 940 and had reported viscosity of 5,180 ± 96 cP, pH of 5.76 ± 0.05 and drug content of 98.16 ± 0.54%. Reported 12-hour release was 96.18 ± 0.54% through egg membrane. Recalculation reproduced the principal full-profile kinetic fits; an early-profile power-law fit gave an exponent of 0.7335. The five-point calibration equation differed from the equation printed in the thesis. The reported series identifies TF8 and TG2 as candidates for experimental confirmation. Primary-record verification, analytical reconciliation and skin-specific testing are required before claims of enhanced cutaneous delivery, therapeutic benefit or shelf life can be supported.

Keywords: *Ruxolitinib; Transfersomes; Topical Gel; Physicochemical Characterization; in Vitro Release; Release Kinetics.*

How to Cite: Rahul Dewangan; Dr. Amit Sahu; Arti Solanki; Dr. S. Nayak (2026) Development and Characterization of Ruxolitinib-Loaded Transfersomal Gel: Physicochemical Properties and in Vitro Release. *International Journal of Innovative Science and Research Technology*, 11(11), 2050-2068. https://doi.org/10.38124/ijisrt/26nov1139

I. INTRODUCTION

Ruxolitinib inhibits Janus kinase 1 and 2 and has been developed for local treatment of inflammatory and immune-mediated skin disorders. Its activity in conventional cream formulations provides the appropriate starting point for investigating a new vehicle. Clinical benefit of the molecule is already established in selected settings; the formulation problem is whether a different carrier can provide a reproducible and useful distribution of drug within the intended skin compartments. A laboratory gel therefore needs to be judged by its composition, analytical reliability, physical behavior and delivery measurements before any therapeutic advantage is proposed [1]. Randomized cream trials in atopic dermatitis and vitiligo support the clinical relevance of topical ruxolitinib, while remaining evidence about those tested creams and indications [2,3].

A formulation that releases drug efficiently into a receptor compartment may still perform differently on skin. Local delivery depends on drug leaving the vehicle, partitioning into the stratum corneum and reaching responsive cells in viable tissue. Drug retained in the vehicle, deposited within skin and recovered beyond the membrane represents different quantities. Maximizing one of these endpoints does not necessarily improve another. Systemic exposure also depends on the formulation and application conditions, so the pharmacokinetic profile of an established cream cannot be transferred to an experimental vesicular gel solely because both contain ruxolitinib [4].

Transfersomes combine phospholipids with an edge activator intended to alter bilayer flexibility. The early vesicle literature proposed a role for hydration forces and transdermal osmotic gradients in transport through skin [5].

ISSN No:-2456-2165 https://doi.org/10.38124/ijisrt/26nov1139

That mechanism supplies a reason to investigate the carrier, but it requires an appropriate barrier model and evidence that the prepared system has the relevant properties. Size, size distribution and electrophoretic behavior characterize a dispersion; they do not by themselves demonstrate deformability, vesicle passage through intact stratum corneum or localization of the active ingredient. These distinctions are necessary when transferring a vesicle concept into a semisolid dosage form.

Published transfersomal gel work with asiatic acid and formulation optimization with ibuprofen show that lipid composition, surfactant selection and gel incorporation can be studied together [6,7]. Their findings help identify variables for experimentation. They do not predict the performance of ruxolitinib, whose ionization, material form, drug-lipid association and analytical response must be established in its own formulation. Ruxolitinib nanoliposomes have also been investigated, including an emulgel formulation, providing direct drug-specific precedent for lipid-based delivery research [8]. A nanoliposome, however, should retain its reported carrier classification unless an edge-activated composition and functional deformation measurements support a transfersomal designation.

The present formulation work used soya phosphatidylcholine, Tween 80 and ethanol to define a vesicle series, followed by Carbopol 940 gels with different polymer concentrations. This creates two related questions. The first concerns selection of a dispersion with an acceptable particle profile and reported drug association. The second concerns the effect of gel structure on handling and release. A candidate that performs favorably in the first stage may change after gel incorporation, making direct measurements of the final product necessary. Screening across several endpoints is useful, provided that the selection rule and uncertainty are made explicit.

For a local formulation, the relevant product question is the relationship between drug availability and the compartment in which activity is intended. Drug detected beyond a membrane is analytically accessible, whereas drug associated with the carrier or retained within a barrier may require separate extraction. These measurements answer different questions. A formulation can therefore give a high receptor recovery without demonstrating improved local targeting. The development rationale for ruxolitinib cream emphasizes local delivery, making compartment-specific assessment a more useful basis for comparison than a general preference for the smallest carrier or fastest release profile [1]. In the present evaluation, release into the receptor is treated as a formulation-performance observation, with no conversion into a therapeutic endpoint.

The experimental sequence also contains two distinct material transitions: preparation of a vesicular dispersion and incorporation of that dispersion into a polymeric vehicle. Measurements made before the second transition do not automatically describe the finished gel. Dilution, mixing and changes in the surrounding medium may alter the state in which drug and vesicles are presented to the membrane. This possibility is a formulation hypothesis rather than an observed change in the current series. Separating dispersion selection from final-gel assessment makes the interpretation more precise: TF8 is the candidate dispersion, while TG2 is one polymer concentration evaluated after incorporation. Their selection requires agreement among composition, assay basis and product performance, rather than a shared designation as optimized.

The objective was to describe the formulation system and assess the reported preformulation, vesicle, gel, diffusion and short-term storage findings without losing their experimental context. The numerical series were also examined for internal agreement and reproducibility of derived calculations. The source thesis identifies several result sets as illustrative or preliminary. That qualification is retained throughout the interpretation. The study therefore supports a formulation-development hypothesis and a defined verification pathway, while leaving enhanced skin delivery and clinical effectiveness to experiments that directly measure those outcomes.

II. MATERIALS AND METHODS

➢ *Materials*

Ruxolitinib was obtained from Bioplus Life Sciences Pvt. Ltd., Bangalore, and soya phosphatidylcholine from Ash Chemie India, Thane. Carbopol 940 was used as the gelling agent, while Tween 80 served as the edge activator. Glycerin and propylene glycol were included in the gel formulation. Other chemicals included phosphate salts, sodium hydroxide, methanol, ethanol and chloroform. The reported suppliers and material details were retained as available in the original thesis.

➢ *Equipment*

The instruments used included a UV-visible spectrophotometer (Labindia 3000+), FTIR spectrometer (Bruker), mechanical stirrer, zeta sizer (Malvern Instruments), microcentrifuge, sonicator, pH meter and Brookfield viscometer. The viscometer was operated using spindle 63 at 10 rpm.

➢ *Preformulation Assessment*

The powder appearance, color, odor and reported taste profile were documented before formulation. The preformulation observations are retained in Table 3. The sensory description was retained as a source observation and was not treated as an analytical identity test. Apparent solubility was examined by adding approximately 1-2 mg of drug separately to 5 mL of water, 0.1 N hydrochloric acid, ethanol, methanol, chloroform, phosphate buffer at pH 7.4 and 0.1 N sodium hydroxide. The mixtures were shaken and observed at room temperature. Equilibration time, residual-solid assessment and measured equilibrium concentrations were not specified. The categorical descriptions were consequently preserved without conversion into quantitative solubility values.

ISSN No:-2456-2165 https://doi.org/10.38124/ijisrt/26nov1139

Table 1 Preformulation Observations

Test	Parameter or medium	Reported observation
Physical description	Color	White to off-white
Physical description	Odor	Odorless
Physical description	Appearance	Crystalline powder
Physical description	Taste profile	Bitter
Apparent solubility	Water	Freely soluble
Apparent solubility	0.1 N HCl	Freely soluble
Apparent solubility	Ethanol	Soluble
Apparent solubility	Methanol	Soluble
Apparent solubility	Chloroform	Slightly soluble
Apparent solubility	Phosphate buffer pH 7.4	Freely soluble
Apparent solubility	0.1 N NaOH	Soluble
Melting interval	Sample	84-86 °C
Melting interval	Reported comparison interval	84-89 °C
Loss on drying	Reported percentage	0.274 ± 0.002%

Solubility categories describe qualitative visual observations, not measured equilibrium concentrations. The material was also described as yellow in the identification record. The loss-on-drying denominator and active-material identity require confirmation; the definition of the ± term and replicate count were not stated.

Melting behavior was described using a capillary or fusion tube in a melting-point apparatus with an oil bath. The reported sample interval and the comparison interval printed in the thesis were retained. Loss on drying was described for approximately 1 g of powder at 100-105 °C for 15 minutes using an infrared moisture balance. The stated result was retained, although initial and final masses were unavailable. The conventional wet-mass expression is shown in Equation 1. The denominator printed in the thesis differed from that expression, so the numerical result could not be independently reconstructed.

$$LOD\ (\%) = \frac{m_i - m_f}{m_i} \times 100 \quad (1)$$

In Equation 1, m_i and m_f denote the initial and final sample masses. No revised loss-on-drying value was generated from an assumed mass. Fourier-transform infrared spectroscopy was used for drug identification, with a Bruker instrument identified in the equipment list. The source spectrum and its assignments were retained in Figure 1 and Table 2. Spectral preparation, resolution, scan count and blank subtraction were not supplied. Separate spectra of blank vesicles, drug-excipient mixtures and the final loaded gel were not available, so a compatibility experiment was not inferred from the drug spectrum alone.

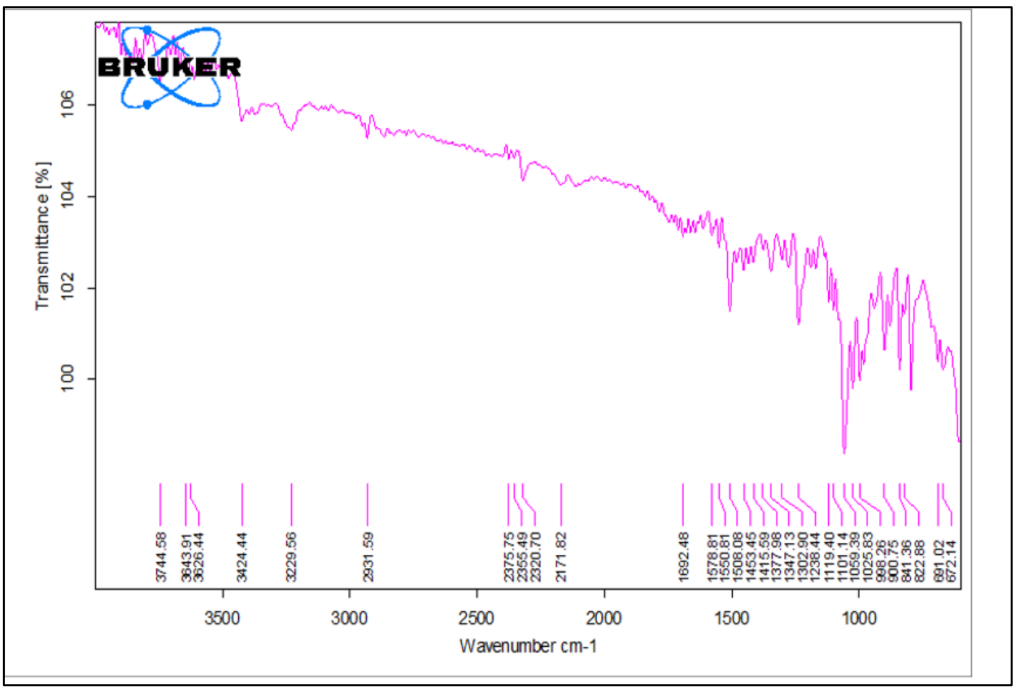


Fig 1 FTIR Spectrum of the Drug Material. The Trace, Peak Labels and Original Transmittance Scale are Retained without Smoothing or signal reconstruction. Separate blank-carrier and mixture spectra were unavailable; the displayed spectrum therefore does not establish drug-excipient compatibility. Primary electronic records and sample identity require confirmation.

ISSN No:-2456-2165 https://doi.org/10.38124/ijisrt/26nov1139

Table 2 FTIR Band Positions and Tentative Assignments

Band assignment	Stated position (cm^{-1})	Tentative interpretation
N-H stretching	3424.44	N-H group in fused nitrogen-containing ring
Aliphatic C-H stretching	2931.59	Cyclopentyl and aliphatic groups
C≡N stretching	2320.70	Tentative nitrile assignment; not independently established
C=N stretching	1692.48	Nitrogen-containing heteroaromatic rings
C=C stretching	1578.81	Aromatic or heteroaromatic skeletal vibration
C-N stretching	1347.13	Nitrogen-containing heterocycles
C-H bending	1415.59	Aliphatic C-H groups
Aromatic C-H out-of-plane bending	841.36	Heteroaromatic C-H deformation

Values denote individual band positions. Functional-group assignments are tentative and have not been independently confirmed. Only the drug spectrum was available; blank-vesicle, mixture and final-gel spectra were not provided.

➢ *Ultraviolet Analysis and Calibration*

A stock solution was described by dissolving 10 mg of drug in 10 mL of methanol, giving a nominal concentration of 1,000 µg/mL. A diluted solution at 10 µg/mL was scanned over 200-400 nm using a Labindia 3000+ spectrophotometer. The reported absorption maximum was 256 nm. For calibration, a 1 mL aliquot of the stock was diluted to 10 mL, after which 0.5, 1.0, 1.5, 2.0 and 2.5 mL aliquots were each diluted to 10 mL with phosphate buffer at pH 7.4. The nominal calibration concentrations were 5, 10, 15, 20 and 25 µg/mL.

The five reported mean absorbances in Table 3 were fitted by unweighted ordinary least squares with a freely estimated intercept. Only the five listed nonzero standards were used in the principal recalculation. A zero standard was not added to improve agreement with the printed graph because no measured blank value was tabulated. The reported mean ± standard deviation values were preserved, with n = 3 retained for this table as explicitly stated in the thesis. Matrix specificity, recovery, intermediate precision, robustness and stability-indicating performance were not established from these five calibration means. The validation framework in Q2(R2) and analytical-development principles in Q14 were used to distinguish calibration from a fully characterized assay [9,10].

The analytical chain was considered at the level of sample preparation as well as regression. A reported percentage depends on the weighed sample basis, extraction volume, subsequent dilution and the response assigned to that diluted extract. An error at any of these stages can produce an apparently precise final percentage. The available mean absorbances allow the calibration calculation to be checked, but they do not reveal whether an extract was completely recovered or whether an excipient contributed to the signal. Analytical validation and procedure development address related but distinct questions [9,10]. Here, this distinction is used to identify which parts of the measurement chain are documented and which remain unresolved; it does not retrospectively validate an assay from its calibration coefficient.

Table 3 Calibration Standards at 256 nm in Phosphate Buffer pH 7.4

Concentration (µg/mL)	Mean absorbance	Reported SD
5	0.145	0.008
10	0.278	0.003
15	0.453	0.005
20	0.602	0.004
25	0.735	0.003

Values are mean and reported SD; n = 3. The reported equation was A = 0.029 C - 0.004, with 0.998 labeled as a correlation coefficient in the tabulation and R^2 in the graph. Re-fitting the five nonzero means gave A = 0.03008 C - 0.00860; R^2 = 0.997919; Pearson r = 0.998959. A measured blank and the unknown-sample absorbances were unavailable.

➢ *Vesicle Formulation Design and Preparation*

The fourteen compositions are reproduced in Table 4. Soya phosphatidylcholine ranged from 100 to 250 mg, ethanol from 5.0 to 10.0 mL and Tween 80 from 10.0 to 20.0 mg, with 10 mg of ruxolitinib listed for every composition. TF13 and TF14 included intermediate ethanol and surfactant levels. Lipid-to-surfactant mass ratios were calculated directly from these ingredient quantities and were identified as derived quantities. A named factorial design, randomization scheme, independent batch replication and fitted response surface were not documented; the series was therefore treated as a formulation screen.

Table 4 Vesicle Composition Matrix

Code	Soya PC (mg)	Ethanol (mL)	Tween 80 (mg)	Drug (mg)	Lipid to Tween mass ratio
TF1	100	5	10	10	10:1
TF2	100	7.5	15	10	6.667:1

ISSN No:-2456-2165 https://doi.org/10.38124/ijisrt/26nov1139

TF3	100	10	20	10	5:1
TF4	150	5	15	10	10:1
TF5	150	7.5	20	10	7.5:1
TF6	150	10	10	10	15:1
TF7	200	5	20	10	10:1
TF8	200	7.5	10	10	20:1
TF9	200	10	15	10	13.33:1
TF10	250	5	10	10	25:1
TF11	250	7.5	15	10	16.67:1
TF12	250	10	20	10	12.5:1
TF13	150	6.25	12.5	10	12:1
TF14	200	8.75	17.5	10	11.43:1

PC, phosphatidylcholine. The active-material salt form remains unconfirmed. Lipid-to-Tween mass ratios are calculated from ingredient inputs. Ethanol volumes denote solvent input rather than measured residual solvent. Hydration volume and final dispersion yield were not available.

Thin-film hydration was described in the thesis. Phospholipid and ruxolitinib were dissolved in ethanol, Tween 80 was added, and the organic phase was mixed. The solvent was removed from a round-bottom flask, followed by drying and hydration of the resulting lipid film. Although the procedure was called a hand-shaking method, reduced-pressure rotary evaporation was also described. The precise operation used for the experimental batches, evaporation temperature, pressure, rotation speed, drying duration, hydration volume and hydration temperature were not supplied. Sonication equipment appeared in the instrument list, but batch-specific sonication settings were absent. These process variables were left unspecified rather than assigned customary laboratory values.

➢ *Vesicle Characterization and Drug Association*

Mean vesicle size and polydispersity index were described as determined by dynamic light scattering, and zeta potential was estimated from electrophoretic mobility. The source named a Malvern Zetamaster ZEM 5002 and a field strength of 20 V/cm. Dilution with 0.9% sodium chloride and an additional conductivity specification were also stated. The conductivity notation in the methods was not sufficiently clear to reconcile with the 0.105 mS/cm displayed in the selected instrument image. Measurement temperature, scattering angle, viscosity input and replicate acquisition scheme were not available. The outputs were consequently interpreted as the reported particle measurements, with attention to their method dependence [11].

For entrapment assessment, 1 mL of suspension was described as centrifuged at 15,000 rpm for 1 hour. The sediment was lysed with methanol and analyzed at 256 nm after supernatant removal. The thesis then printed a difference-based equation using theoretical and practical drug content. Because sediment analysis and supernatant analysis require different numerator definitions, both operational expressions are shown in Equation 2. The reported entrapment values were not silently recalculated using an assumed fraction. Rotor radius, relative centrifugal force, separation recovery, free-drug carryover and individual assay readings were unavailable.

$$EE\ (\%) = \frac{M_{total} - M_{free}}{M_{total}} \times 100 \quad (2a)$$

$$EE\ (\%) = \frac{M_{associated}}{M_{total}} \times 100 \quad (2b)$$

Here, M_{total} is the relevant total drug amount, M_{free} is drug measured in the unentrapped fraction, and $M_{associated}$ is drug recovered from the separated vesicular fraction. Verification of the assayed fraction and recovery is required before either expression can be assigned to the experiment.

➢ *Gel Preparation and Evaluation*

A hydrated Carbopol 940 base was prepared in purified water. Glycerin and propylene glycol were incorporated with gentle stirring before the transfersomal dispersion was added. Triethanolamine was described as added dropwise to adjust consistency and pH, and water was added to a final mass of 100 g. TG1, TG2 and TG3 contained 0.5%, 0.75% and 1.0% Carbopol 940, respectively, with glycerin and propylene glycol each listed at 5% w/w (Table 5). The intended ruxolitinib strength was 1.5% w/w, expressed as a dispersion quantity equivalent to that drug content. Exact dispersion concentration and incorporation volume were not provided, so the final drug mass balance could not be reconstructed from the 10 mg vesicle-scale entries alone.

Table 5 Gel Compositions

Ingredient or basis	**TG1**	**TG2**	**TG3**
Ruxolitinib-loaded dispersion	Equivalent to 1.5% drug	Equivalent to 1.5% drug	Equivalent to 1.5% drug
Carbopol 940 (% w/w)	0.5	0.75	1.0
Glycerin (% w/w)	5	5	5
Propylene glycol (% w/w)	5	5	5
Triethanolamine	q.s. to target pH	q.s. to target pH	q.s. to target pH

ISSN No:-2456-2165 https://doi.org/10.38124/ijisrt/26nov1139

Purified water	q.s. to 100 g	q.s. to 100 g	q.s. to 100 g

q.s., quantity sufficient. The intended drug strength is 1.5% w/w of final gel. The incorporated dispersion concentration, volume and scaling or concentration history were not documented, leaving the final dose mass balance unresolved.

Viscosity was described using a Brookfield viscometer with spindle 63 at 10 rpm. Measurement temperature, equilibration and instrument model were not recorded. The result was treated as a single-condition apparent viscosity rather than a complete flow curve. The pH meter was described as calibrated with buffers at pH 4, 7 and 9.2. For drug content, the wording specified an amount equivalent to 100 mg of gel, extraction with 20 mL methanol, filtration through Whatman No. 1 paper, and dilution of 1 mL filtrate to 10 mL. The ambiguity between gel mass and drug-equivalent mass was retained as an assay limitation.

Extrudability was expressed as the mass expelled divided by the initial gel mass in the tube, multiplied by 100. Tube geometry, applied load and extrusion time were not specified. Spreadability was described using approximately 2-5 g gel between slides, a 20 g load and 6 cm movement. The relation S = mL/t was used, where m is the applied mass, L the travel distance and t the slide transit time. The supplied spreadability values were retained with units of g cm/s. Neither test was interpreted as a direct measurement of skin adhesion or clinical acceptability.

➢ *In Vitro Diffusion and Release Assessment*

A Franz-type cell with an approximately 60 mL receptor compartment and a stated diffusion area of 3.14 cm² was described. Egg membrane separated donor and receptor compartments. Phosphate buffer at pH 7.4 was maintained at 32 ± 0.5 °C with magnetic stirring. Samples were withdrawn and replaced by equal volumes of fresh receptor medium, and absorbance was measured at 256 nm. Results were tabulated at 0.5, 1, 2, 3, 4, 5, 6, 8, 10 and 12 hours. Donor gel mass, sampling volume, membrane pretreatment and demonstrated sink conditions were not documented. The methods also referred to a 2 cm² patch, leaving an unresolved inconsistency with the gel dosage form and stated cell area.

For constant receptor volume and repeated replacement with drug-free medium, the sampling-corrected recovered amount can be written as Equation 3. The equation identifies the data needed for verification; no recovered mass or flux was calculated because the individual concentrations and sampling volume were absent.

$$Q_n = V_r C_n + V_s \sum_{i=1}^{n-1} C_i \quad (3)$$

In Equation 3, V_r is receptor volume, C_n is the concentration at the current sampling point, V_s is sampling volume, and the sum contains concentrations at earlier withdrawals. Percent release additionally requires a verified applied drug amount. The tabulated percentages were retained as reported. Egg membrane was treated as a diffusion barrier rather than human or animal skin. The assay was not described as a validated regulatory IVRT comparison or a skin-absorption study [12,13].

➢ *Release-Kinetic Analysis*

The TG2 mean percentages were examined using zero-order, first-order, square-root-of-time and power-law transformations. Full-profile ordinary least squares fits were performed for comparison with the published thesis plots. Intercepts were estimated rather than forced to zero, and the ten reported nonzero time points were retained. The transformed expressions are shown in Equation 4. The coefficient of determination described fit in the transformed response space for each model and was not treated as a directly comparable error measure across all transformations.

$$Q_t = a_0 + k_0 t \quad (4a)$$

$$log_{10}(100 - Q_t) = a_1 + bt \quad (4b)$$

$$Q_t = a_H + k_H \sqrt{t} \quad (4c)$$

$$log_{10} Q_t = a + n \, log_{10} t \quad (4d)$$

Q_t denotes reported cumulative percentage release at time t. For the power-law expression, n is the fitted slope and a is the intercept when percentage release is used. The empirical framework originates in polymer-release studies and depends on its applicable geometry and release interval [14,15]. An additional exploratory fit was therefore restricted to the five reported points through 4 hours, for which TG2 release remained below 60%. This range restriction was a manuscript-stage reanalysis of the supplied mean series, not a new experiment. Higuchi interpretation was also kept separate from proof of a physical diffusion mechanism [16].

➢ *Short-Term Storage and Statistical Treatment*

TG2 was described as stored in borosilicate containers under refrigeration at 4.0 ± 0.2 °C and at room temperature for three weeks. The room-temperature notation was printed as 25-28 ± 2 °C and was retained without inventing a controlled set point. Appearance, homogeneity, phase separation and drug content were recorded at Day 0 and Weeks 1, 2 and 3. Humidity, light exposure, closure details and stability-assay specificity were not established. The study was treated as short-term observation, not a shelf-life determination [17].

Descriptive values were preserved at their reported precision. The calibration and entrapment tables explicitly indicated three determinations with standard deviations. For other tables, ± terms were retained as reported, without assigning an undocumented replicate count or uncertainty definition. Single displayed size and zeta values were not given invented error bars. No hypothesis test, p value or confidence interval was calculated from unavailable individual replicates. Derived fits and arithmetic comparisons were calculated from transcribed values using Python and NumPy. Such calculations establish numerical consistency

ISSN No:-2456-2165 https://doi.org/10.38124/ijisrt/26nov1139

with the reported series, while leaving the provenance and reproducibility of the laboratory observations unresolved.

Additional descriptive comparisons were calculated directly from the listed means. Relative differences in gel attributes used the initial formulation mean as the denominator and were kept separate from absolute percentage-point differences. Times at which the mean release profiles crossed 50% and 80% were estimated by straight-line interpolation between the two adjacent sampling times that bracketed each threshold. No time-zero value was added and no extrapolation outside the observed interval was performed. These interpolated times are summaries of the reported profiles, not independently observed sampling events, kinetic half-lives or estimates with established confidence intervals. They inherit the illustrative status of the input series and do not supply evidence of statistical separation between formulations.

III. RESULTS

➢ *Preformulation Observations and Spectral Record*

The preformulation record described a white to off-white, odorless crystalline powder with a bitter taste profile. A later identification paragraph described the material as yellow, creating an unresolved inconsistency in the source description. The measured melting interval was reported as 84-86 °C, compared with a printed reference interval of 84-89 °C. Loss on drying was reported as 0.274 ± 0.002%. These observations are retained in Table 3. They provide a description of the supplied material, while the conflicting color descriptions and unconfirmed material form prevent an identity conclusion based on appearance and melting behavior alone.

The solubility screen classified the drug as freely soluble in water, 0.1 N hydrochloric acid and phosphate buffer at pH 7.4; soluble in ethanol, methanol and 0.1 N sodium hydroxide; and slightly soluble in chloroform. The experiment used a very small nominal solute mass relative to solvent volume. Visual dissolution at that ratio does not locate the equilibrium solubility or substantiate the printed pharmacopoeial category. The original classifications were therefore retained as qualitative source descriptions, with no numerical solubility inferred from them.

The FTIR table listed bands at 3424.44, 2931.59, 2320.70, 1692.48, 1578.81, 1347.13, 1415.59 and 841.36 cm^{-1}. The spectrum is reproduced without reconstruction in Figure 1, and the complete source assignment list is retained in Table 4. The 2320.70 cm^{-1} band was assigned to nitrile stretching by the thesis; that assignment was not independently verified. The presence of a drug-only spectrum did not establish absence of drug-excipient interaction because no corresponding blank or mixture spectra were supplied. The spectrum was consequently used as an identification exhibit of unresolved provenance, with its original axes and labels preserved.

➢ *Ultraviolet Response and Calibration Agreement*

The displayed ultraviolet scan had a labeled maximum at 256 nm. Across the five tabulated standards, mean absorbance increased from 0.145 ± 0.008 at 5 µg/mL to 0.735 ± 0.003 at 25 µg/mL. All five concentration-response pairs and their stated standard deviations are included in Table 5. Figure 2 retains the source ultraviolet scan and presents a fresh plot of the numerical standards, with error bars corresponding to the reported standard deviations.

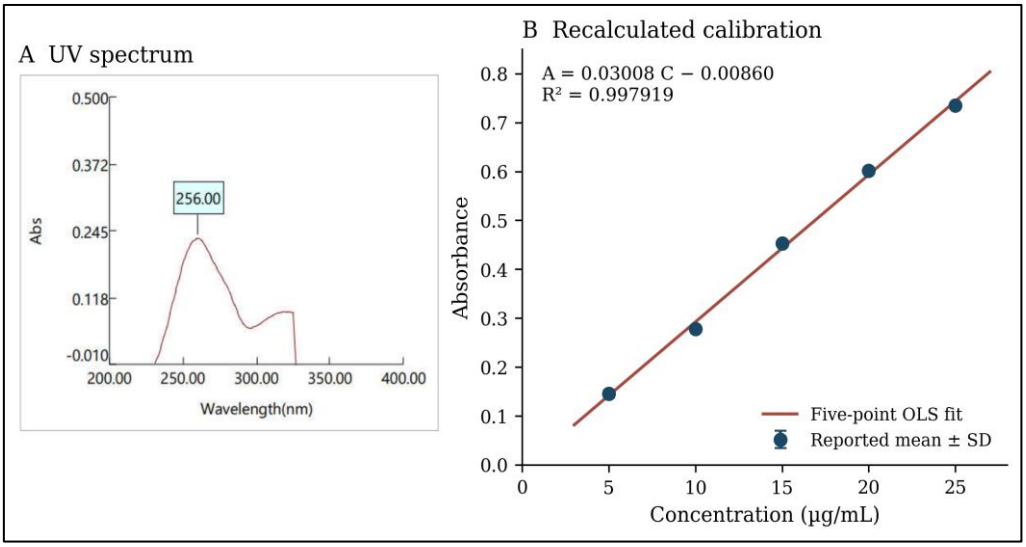


Fig 2 Ultraviolet Spectrum and Calibration Response. (A) UV Scan with a Labeled Maximum at 256 nm. (B) Five Calibration Means with Reported SD bars (n = 3). The Line is the Recalculated Five-Point Ordinary least Squares fit, A = 0.03008 C - 0.00860; R^2 = 0.997919. No Unreported zero Standard was Added. The Recalculated fit Differs from the Previously Reported Regression Annotation.

The recalculated five-point relation was A = 0.03008C - 0.00860, where A is absorbance and C is nominal concentration in µg/mL. The coefficient of determination was 0.997919, and the Pearson correlation coefficient was 0.998959. The thesis printed A = 0.029C - 0.004 and reported 0.998, labeling the statistic as a correlation coefficient in its

ISSN No:-2456-2165 https://doi.org/10.38124/ijisrt/26nov1139

table and R^2 in its graph. These alternatives are shown separately. The original graph also displayed a zero point without a listed blank absorbance. No such point was introduced into the principal recalculation.

The five means support a nearly linear relationship over the tested nominal range. They do not establish that every sample matrix could be quantified without interference. Because the reported entrapment fraction was lysed in methanol and gel assays were also described in methanol, the relationship between those assay media and the phosphate-buffer calibration remains important. Absorbance readings for the unknowns and their complete dilution records were unavailable, so the effect of the calibration discrepancy on the reported drug-content and entrapment values was not estimated.

➢ *Formulation Composition and Vesicle Measurements*

The ingredient matrix covered lipid-to-Tween 80 mass ratios from 5:1 to 25:1. TF8 contained 200 mg soya phosphatidylcholine, 10 mg Tween 80, 7.5 mL ethanol and 10 mg ruxolitinib, corresponding to a lipid-to-surfactant mass ratio of 20:1. TF14 contained the same listed lipid and drug masses, with 17.5 mg Tween 80 and 8.75 mL ethanol. Composition is presented separately from response data so that the identity of each formulation is retained when the numerical endpoints are compared.

Mean vesicle sizes ranged from 148.6 nm for TF8 to 196.8 nm for TF3. The corresponding PDI range was 0.198-0.312. All reported zeta potentials were negative, from -26.2 mV for TF8 to -17.2 mV for TF3. TF8 therefore occupied the favorable end of the reported size, PDI and zeta-potential series simultaneously, while TF14 and TF5 also had comparatively low sizes and PDIs. Table 6 preserves every formulation-level value. Figure 3 presents the three endpoints in separate panels with their own axes, avoiding the mixed-unit scale of the original combined chart.

Table 6 Vesicle Characteristics and Reported Entrapment

Code	Reported size (nm)	PDI	Zeta potential (mV)	Entrapment (%)
TF1	185.6	0.284	-18.6	72.45 ± 0.98
TF2	172.4	0.261	-20.3	76.82 ± 0.96
TF3	196.8	0.312	-17.2	68.54 ± 0.75
TF4	168.7	0.238	-22.1	79.36 ± 0.65
TF5	154.2	0.216	-24.5	84.27 ± 0.38
TF6	181.3	0.275	-19.4	75.63 ± 0.66
TF7	162.5	0.229	-23.6	82.15 ± 0.74
TF8	148.6	0.198	-26.2	88.64 ± 0.52
TF9	175.9	0.253	-21.0	77.48 ± 0.63
TF10	177.2	0.267	-20.1	74.92 ± 0.88
TF11	163.8	0.235	-23.0	81.57 ± 0.82
TF12	189.4	0.298	-18.1	70.86 ± 0.63
TF13	159.6	0.224	-24.0	83.42 ± 0.77
TF14	151.8	0.207	-25.1	86.35 ± 0.54

The numerical series is illustrative and requires confirmation against primary laboratory records. Entrapment is reported as mean ± SD from three determinations; independent batch replication was not established. Uncertainty and replicate counts were not given for size, PDI or zeta potential. The assayed drug fraction and entrapment calculation require reconciliation.

The selected size image displayed a Z-average value of 148.60, PDI of 0.198 and intercept of 0.185. Its peak table and intensity distribution are retained in Figure 4A. The zeta image displayed -26.20 mV, zeta deviation of 1.25 mV and conductivity of 0.105 mS/cm, with a peak-width entry of 35.65 mV; the complete image is retained in Figure 4B. Zeta deviation and peak width were not substituted for between-batch uncertainty. The reported size-axis notation was also preserved in the source image rather than relabeled as a verified diameter measurement.

ISSN No:-2456-2165 https://doi.org/10.38124/ijisrt/26nov1139

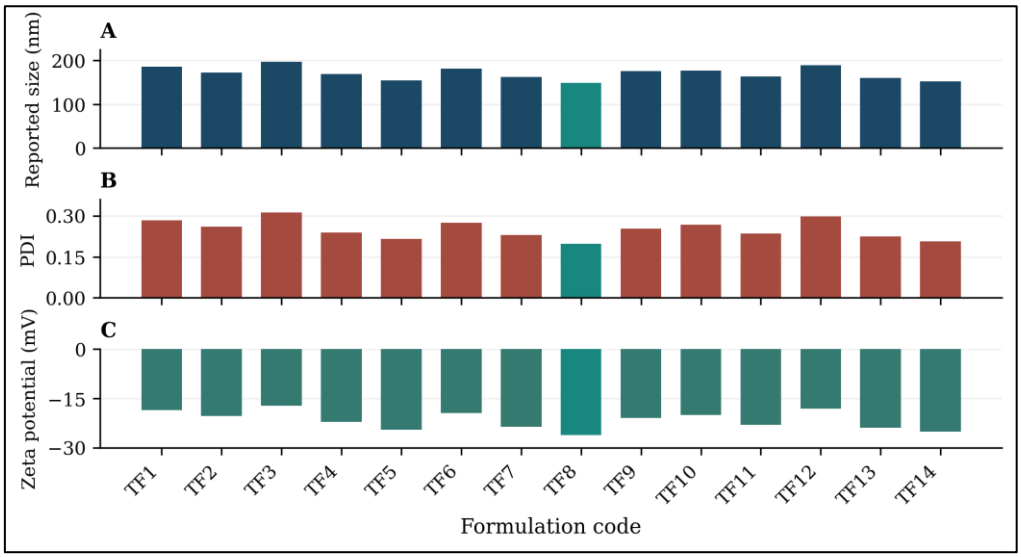


Fig 3 Vesicle Characteristics Across Fourteen Formulations. (A) Reported Mean Size. (B) Polydispersity Index. (C) Zeta Potential. Each Endpoint has its Own Scale and TF8 is Highlighted. Uncertainty was not Provided, so Error Bars are Omitted. The Illustrative Numerical Series Requires Experimental Confirmation.

➢ *Reported Entrapment and Candidate Selection*

The entrapment series ranged from 68.54 ± 0.75% for TF3 to 88.64 ± 0.52% for TF8. TF14 and TF5 followed at 86.35 ± 0.54% and 84.27 ± 0.38%, respectively. The thesis specified three determinations for this table, but did not establish whether they represented repeated readings, separately processed aliquots or independently manufactured batches. All reported values and uncertainties are retained alongside the vesicle measurements in Table 8, and the full entrapment series is shown with the reported standard deviations in Figure 5.

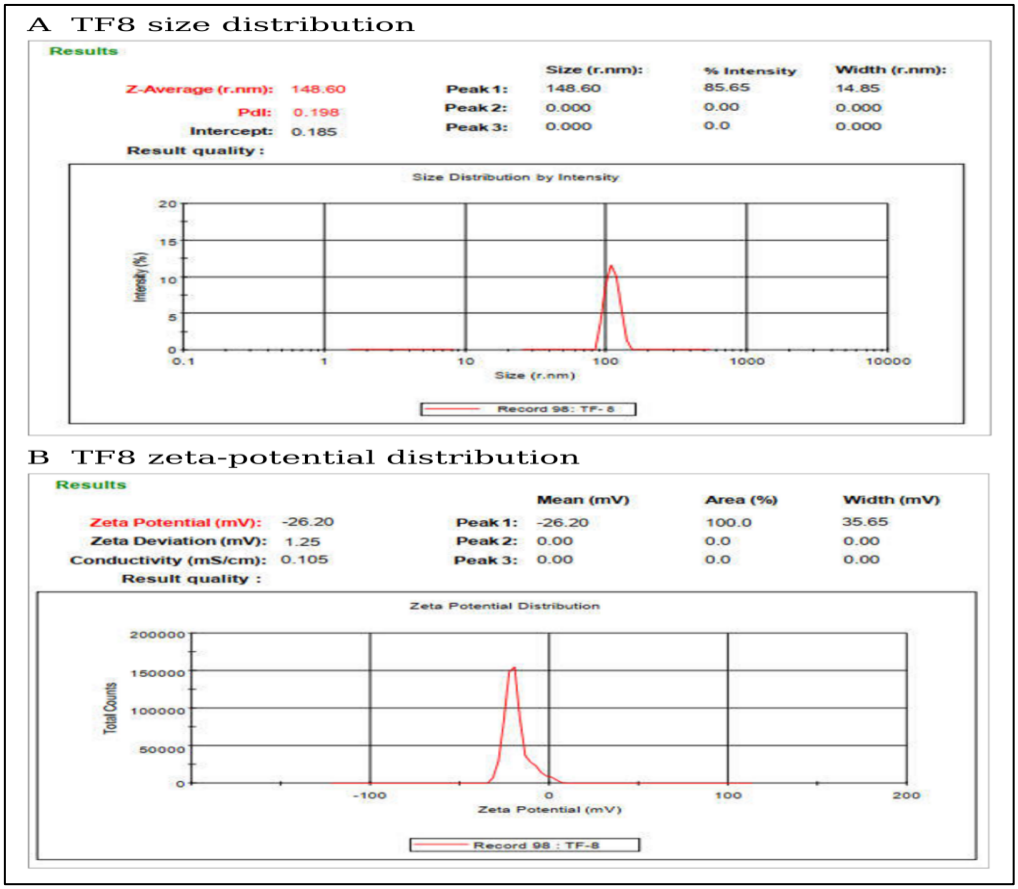


Fig 4 TF8 Particle-Size and Zeta-Potential Distributions. (A) Size-Distribution Output, Including 148.60 and PDI 0.198. (B) Zeta-Potential Output, Including -26.20 mV. The Displayed Axes, Peak Tables, Original Size Notation, blank Result-Quality Fields and Conductivity Output are Retained. The Images do not Replace Verification of the Primary Electronic Measurement Files.

ISSN No:-2456-2165 https://doi.org/10.38124/ijisrt/26nov1139

The difference between the TF8 and TF3 reported means was 20.10 percentage points. This arithmetic comparison describes the supplied series; it was not assigned statistical significance. TF8 was carried forward as a candidate because the same code combined the smallest reported size, lowest PDI and largest reported entrapment value. The unresolved separation-assay definition prevents the percentage from being treated as independently confirmed encapsulation. The candidate designation therefore refers to the screening record, rather than an established manufacturing optimum.

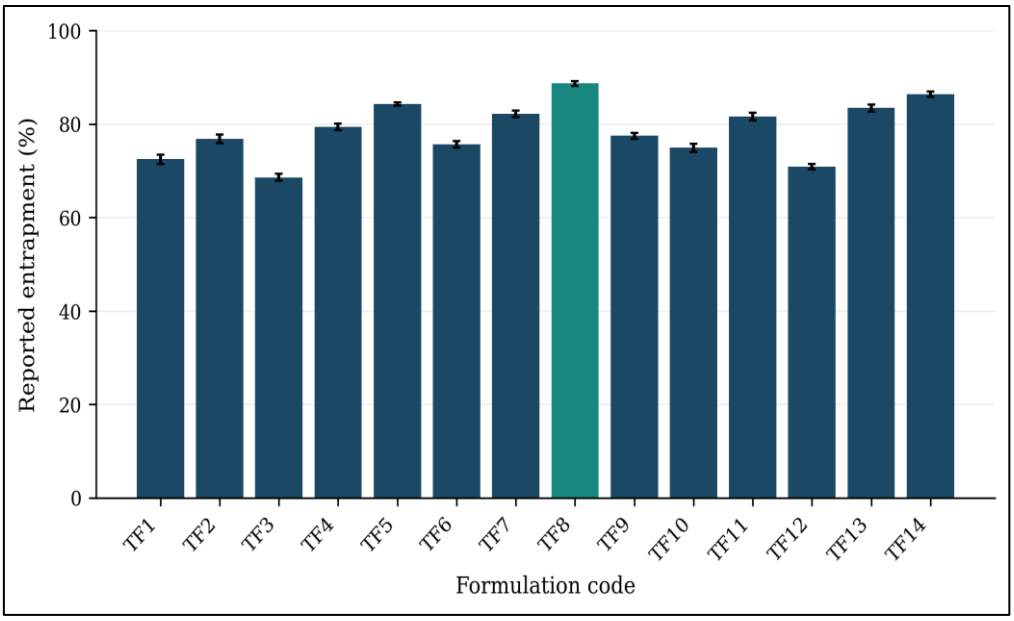


Fig 5 Reported Entrapment Across TF1-TF14. Bars Represent Means with Reported SD from Three Determinations. Independent Batch Replication and the Assayed Drug Fraction were not Established. TF8 is Highlighted within the Illustrative Series; the Graph Does not Imply a Statistically Confirmed Advantage.

➢ *Gel Composition and Physicochemical Properties*

The gel matrix changed Carbopol 940 concentration while retaining the listed glycerin and propylene glycol levels. The complete composition is shown in Table 5. Increasing polymer concentration from TG1 to TG3 coincided with an increase in reported apparent viscosity from 4,250 ± 85 to 6,420 ± 112 cP. Over the same series, spreadability declined from 8.65 ± 0.22 to 7.18 ± 0.17 g cm/s, and extrudability declined from 94.2 ± 1.2% to 87.8 ± 1.6%. These measurements are displayed together in Table 7 and Figure 6, while their distinct units and test definitions are retained.

Table 7 Physicochemical Properties of the Gel Formulations

Attribute	TG1	TG2	TG3
Viscosity (cP)	4,250 ± 85	5,180 ± 96	6,420 ± 112
pH	5.82 ± 0.06	5.76 ± 0.05	5.69 ± 0.04
Drug content (%)	97.42 ± 0.68	98.16 ± 0.54	97.85 ± 0.61
Extrudability (%)	94.2 ± 1.2	91.6 ± 1.4	87.8 ± 1.6
Spreadability (g cm/s)	8.65 ± 0.22	7.92 ± 0.19	7.18 ± 0.17

The ± terms are retained as reported; their statistical definition and replicate counts were not stated. The numerical series forms part of the illustrative evaluation record. Viscosity is a single-condition apparent value. Drug content (%) and intended drug strength (% w/w) express different quantities.

TG2 had an intermediate reported viscosity of 5,180 ± 96 cP, spreadability of 7.92 ± 0.19 g cm/s and extrudability of 91.6 ± 1.4%. Its reported pH was 5.76 ± 0.05, compared with 5.82 ± 0.06 for TG1 and 5.69 ± 0.04 for TG3. Drug content was reported as 97.42 ± 0.68%, 98.16 ± 0.54% and 97.85 ± 0.61% for TG1, TG2 and TG3, respectively. The highest reported content was therefore associated with TG2, whereas the fastest extrusion and spreading were associated with TG1.

ISSN No:-2456-2165 https://doi.org/10.38124/ijisrt/26nov1139

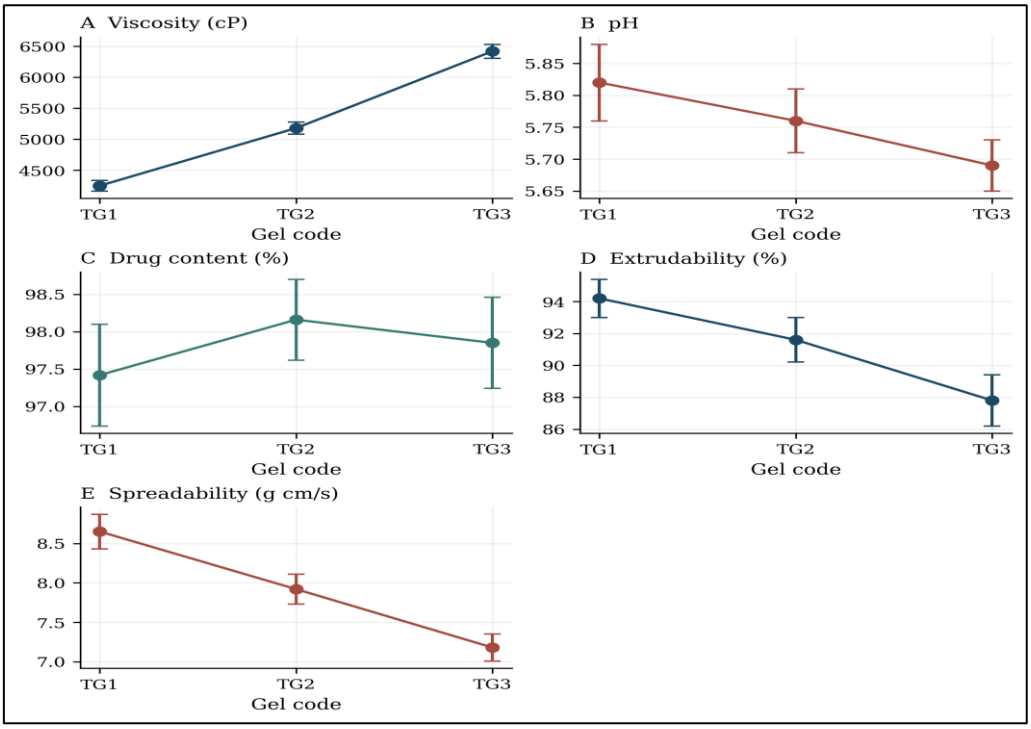


Fig 6 Physicochemical Comparison of TG1, TG2 and TG3, Containing 0.5%, 0.75% and 1.0% Carbopol 940, Respectively. Panels show Apparent Viscosity, pH, Drug Content, Extrudability and Spreadability. Error Bars Retain the Reported ± Terms, Whose Statistical Basis and Replicate Counts were not Specified. The Measurements do not Establish Clinical Acceptability or Skin Residence.

This pattern supports treating selection as a trade-off among measured attributes. No documented acceptance limits or numerical weighting scheme established that the intermediate formulation was superior overall. Drug content represented the reported recovery relative to its stated basis, not a demonstrated content-uniformity study across sampling positions or manufactured batches. The intended 1.5% drug strength and percentage-of-label recovery also remained different quantities and were not interchanged.

Using TG1 as the descriptive baseline, the TG3 viscosity mean was 51.06% higher, while its spreadability mean was 16.99% lower. Extrudability decreased by 6.4 percentage points over the same comparison. These quantities have different denominators: a relative percentage change in viscosity is not equivalent to a percentage-point difference in extrusion. The pH means differed by 0.13 units between TG1 and TG3. TG2 drug content exceeded TG1 by 0.74 percentage points, a much smaller numerical contrast than the viscosity change. Because uncertainty definitions and independent replication were not established for these endpoints, the calculations describe the scale of the reported differences without assigning significance or a common performance score. They also show why a formulation ranking depends on the attribute selected for comparison.

➢ *Complete Diffusion Profiles*

All thirty mean release values and their reported ± terms are preserved in Table 8. TG1 exceeded TG2 and TG3 at every listed time point, while TG3 remained lowest. At 0.5 hours, the reported values were 15.24 ± 0.72%, 12.45 ± 0.68% and 10.18 ± 0.64% for TG1, TG2 and TG3. At 6 hours, they were 80.16 ± 0.79%, 74.26 ± 0.83% and 68.52 ± 0.81%. By 12 hours, they reached 98.26 ± 0.48%, 96.18 ± 0.54% and 93.72 ± 0.58%, respectively. Figure 7 uses the listed nonzero sampling times and preserves the full profiles.

Table 8 Cumulative Release Through Egg Membrane

Time (h)	TG1 (%)	TG2 (%)	TG3 (%)
0.5	15.24 ± 0.72	12.45 ± 0.68	10.18 ± 0.64
1	25.86 ± 0.81	21.38 ± 0.74	18.42 ± 0.71
2	39.72 ± 0.94	34.62 ± 0.89	29.85 ± 0.82
3	52.64 ± 0.88	46.75 ± 0.92	41.26 ± 0.86
4	63.48 ± 0.91	57.84 ± 0.86	51.72 ± 0.93
5	72.35 ± 0.84	66.93 ± 0.78	60.84 ± 0.87
6	80.16 ± 0.79	74.26 ± 0.83	68.52 ± 0.81
8	89.42 ± 0.73	84.57 ± 0.71	79.64 ± 0.76
10	96.45 ± 0.61	91.32 ± 0.65	87.46 ± 0.69
12	98.26 ± 0.48	96.18 ± 0.54	93.72 ± 0.58

ISSN No:-2456-2165 https://doi.org/10.38124/ijisrt/26nov1139

Values are reported cumulative release means with their original ± terms. The uncertainty definition and replicate structure were not specified. The endpoint is release through egg membrane; it does not quantify cutaneous flux or skin retention. Donor-dose and sampling-volume records were unavailable.

TG2 release was 6.12 percentage points above TG3 at 4 hours and 2.46 percentage points above TG3 at 12 hours. The narrowing difference is consistent with the reported curves approaching high cumulative release within the observation window. It does not identify how much drug reached any skin layer. No measured receptor concentrations, donor recovery, membrane recovery or tissue-deposition values accompanied the percentages. A mass-normalized steady-state flux, permeability coefficient or skin-retention percentage could therefore not be derived from the supplied record.

Straight-line interpolation of the reported mean profiles gave approximate 50% crossing times of 2.80, 3.29 and 3.84 hours for TG1, TG2 and TG3, respectively. The corresponding 80% crossing times were 5.98, 7.11 and 8.09 hours. Both summaries retained the same ordering as the tabulated release percentages. Their value is descriptive: they express the separation of the mean curves in time units without selecting a release model. They do not establish a clinically desirable onset or duration, and their precision is limited by the sampling intervals and the unverified experimental provenance. In particular, a threshold falling between two sampling times was calculated from a local straight segment; it was not recorded as a measured event.

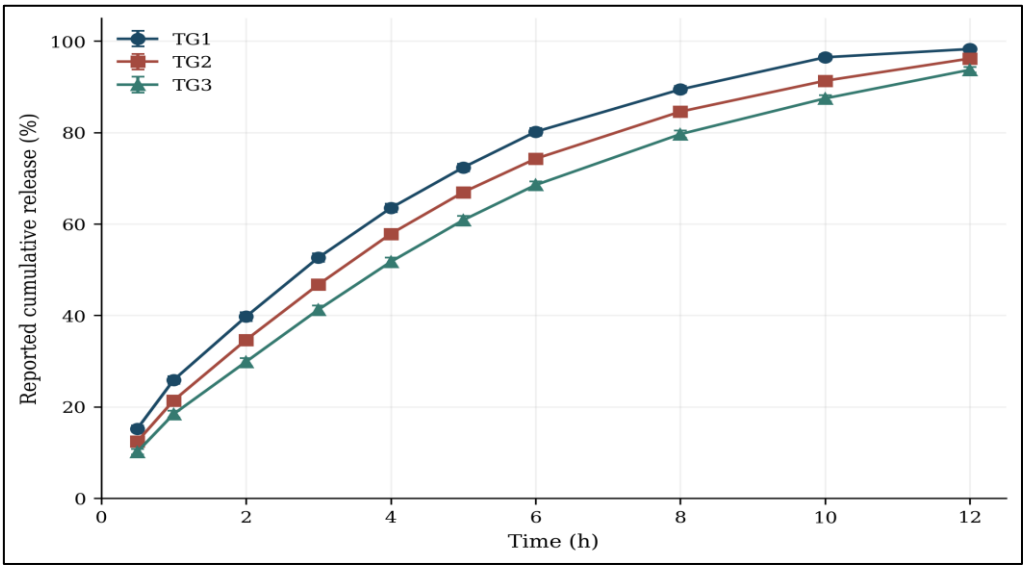


Fig 7 Cumulative Release Profiles Through egg Membrane. All ten Reported Nonzero Sampling Times are Shown for Each gel. Error bars retain the reported ± terms; their definition and replicate Structure were not specified. No Unreported time-zero measurement was introduced. These percentages are not measurements of skin flux, permeability or tissue retention.

➢ *Kinetic Recalculation*

Table 9 retains the complete transformation table printed for TG2. The full-profile zero-order fit gave a slope of 7.2609 percentage points/h, intercept of 21.2364 and R^2 of 0.917274. The first-order transformation gave a slope of -0.114157 h^{-1}, intercept of 2.052255 and R^2 of 0.987335. The square-root-of-time fit gave a slope of 32.0011 percentage points/$h^{1/2}$, intercept of -8.55224 and R^2 of 0.987272. The full-profile power-law transformation gave a slope of 0.657326, intercept of 1.332311 and R^2 of 0.987760. These calculations closely reproduced the values displayed in the thesis, with small differences attributable to calculation from the listed means rather than the rounded transformation columns.

Table 9 TG2 Transformations Used for Release-Model Assessment

Time (h)	$\log_{10}$ t	√t	Release (%)	$\log_{10}$ release	Remaining (%)	$\log_{10}$ remaining
0.5	-0.3010	0.7071	12.45	1.0952	87.55	1.9422
1	0.0000	1.0000	21.38	1.3300	78.62	1.8955
2	0.3010	1.4142	34.62	1.5392	65.38	1.8154
3	0.4771	1.7321	46.75	1.6693	53.25	1.7260
4	0.6021	2.0000	57.84	1.7622	42.16	1.6248
5	0.6990	2.2361	66.93	1.8256	33.07	1.5193
6	0.7782	2.4495	74.26	1.8707	25.74	1.4107
8	0.9031	2.8284	84.57	1.9272	15.43	1.1883
10	1.0000	3.1623	91.32	1.9607	8.68	0.9385
12	1.0792	3.4641	96.18	1.9831	3.82	0.5821

ISSN No:-2456-2165 https://doi.org/10.38124/ijisrt/26nov1139

Transformed values retain their reported numerical precision. Fits in Table 10 were recalculated from the original TG2 mean percentages at full precision. Time is in hours; square-root time has units h^0.5. Logarithms follow the numerical convention used for the reported transformations.

The early-profile power-law fit used the five points from 0.5 through 4 hours, ending at 57.84% reported release. It gave a slope of 0.733470 and R^2 of 0.999606. This result is reported separately from the source full-profile slope of approximately 0.6574. Table 10 distinguishes source fit statistics from the recalculated full-profile and exploratory early-profile values. Figure 8 shows the transformed points and fitted lines. No physical transport mechanism was assigned solely from the largest R^2 or from a release exponent obtained for an incompletely characterized composite vesicle-gel-membrane system.

Table 10 Reported and Recalculated TG2 Regression Statistics

Model	Reported R^2	Recalculated slope	Recalculated intercept	Recalculated R^2	Points
Zero order	0.9173	7.260884	21.236447	0.917274	10
First-order transformation	0.9873	-0.114157	2.052255	0.987335	10
Square-root transformation	0.9873	32.001089	-8.552238	0.987272	10
Power law, full profile	0.9878	0.657326	1.332311	0.987760	10
Power law, early profile	Not reported	0.733470	1.320993	0.999606	5

Reported fit equations: zero order y = 7.2609x + 21.236; first order y = -0.1141x + 2.0521; Higuchi y = 32.001x - 8.5524; power law y = 0.6574x + 1.3322. Full-profile fits use 0.5-12 h. The additional early-profile fit uses five points through 4 h (release ≤ 60%). Recalculated values are derived summaries, not new observations. R^2 values for different response transformations do not alone rank physical mechanisms.

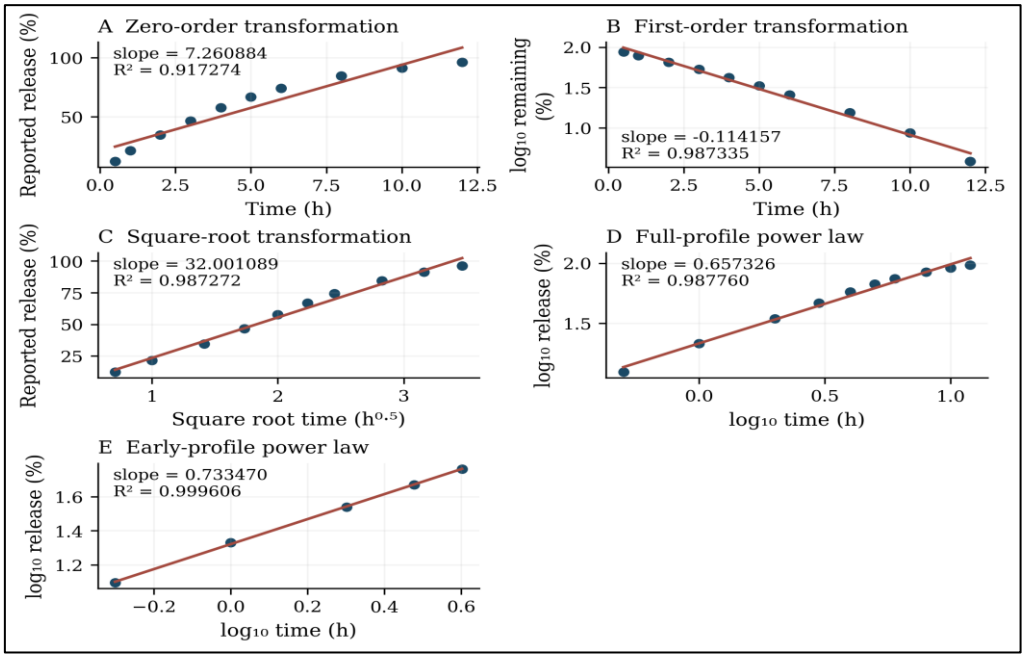


Fig 8 Recalculated TG2 release transformations. (A) Zero order, (B) first order, (C) square-root time and (D) full-profile power law use all ten nonzero time points. (E) The exploratory early-profile power-law fit uses five points through 4 h, with release below 60%. Points are transformed reported means and lines are recalculated regressions. The two power-law exponents are not assigned a unique physical mechanism. Each R^2 refers to its own transformed response space.

➢ *Short-Term Storage Observations*

The complete storage record is retained in Table 11. Both conditions were described as maintaining a smooth, homogeneous gel without visible phase separation over three weeks. Under refrigeration, the reported drug-content series was 98.16%, 98.02%, 97.89% and 97.74%. At room temperature, it was 98.16%, 97.86%, 97.51% and 97.18%. The Week 3 changes were therefore -0.42 and -0.98 percentage points, respectively. Figure 9 presents the listed content values without invented error bars.

Relative to the initial reported content, the corresponding Week 3 retentions were 99.57% and 99.00%, calculated from the tabulated means. These arithmetic retentions were not reported as analytical recoveries or degradation rates. No uncertainty estimates were available for the storage series, and no supporting size, PDI, zeta-potential or release measurements were provided at those storage time points. The observations describe the short interval and tested attributes only. Their illustrative source status and the absence of stability-indicating assay evidence prevent a shelf-life or confirmed chemical-stability conclusion.

ISSN No:-2456-2165 https://doi.org/10.38124/ijisrt/26nov1139

Table 11 TG2 Appearance and Drug Content During three Weeks of Storage

Condition	Attribute	Day 0	Week 1	Week 2	Week 3
Refrigeration	Appearance	Smooth gel	Smooth gel	Smooth gel	Smooth gel
Refrigeration	Homogeneity	Homogeneous	Homogeneous	Homogeneous	Homogeneous
Refrigeration	Phase separation	Absent	Absent	Absent	Absent
Refrigeration	Drug content (%)	98.16	98.02	97.89	97.74
Room condition	Appearance	Smooth gel	Smooth gel	Smooth gel	Smooth gel
Room condition	Homogeneity	Homogeneous	Homogeneous	Homogeneous	Homogeneous
Room condition	Phase separation	Absent	Absent	Absent	Absent
Room condition	Drug content (%)	98.16	97.86	97.51	97.18

Refrigeration was specified as 4.0 ± 0.2 °C. Room temperature was recorded as 25-28 ± 2 °C, without a reconciled controlled set point. The dataset is illustrative; uncertainty and replicate counts were not given. These observations do not establish shelf life.

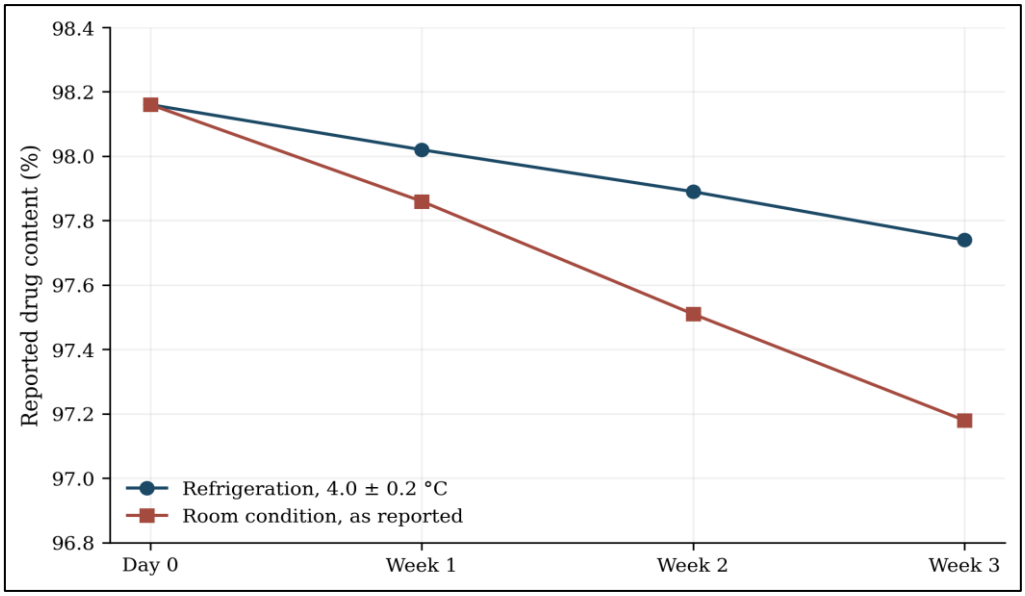


Fig 9 TG2 Drug Content Over three Weeks of Storage. Refrigeration was Recorded as 4.0 ± 0.2 °C; the Room-Temperature notation was 25-28 ± 2 °C. Error bars are omitted because uncertainty and replicate counts were not supplied. The truncated vertical axis makes the small numerical changes visible. The illustrative series does not establish shelf life.

IV. DISCUSSIONS

➢ *What the Formulation Screen Establishes*

The reported series identifies a coherent candidate within the recorded screening space. TF8 had the smallest listed vesicle size and PDI, the most negative zeta potential and the highest reported entrapment. Agreement among these endpoints explains why the formulation was selected for the gel stage. It does not establish a global optimum. Several ingredient quantities changed together, and the source did not provide a fitted design model, independent confirmation batches or a prespecified desirability function. The appropriate conclusion is that TF8 warrants confirmation under a defined manufacturing procedure.

The distinction between a candidate and an optimum is consequential for how the screening results can be used. A candidate is the formulation chosen for a defined next experiment; an optimum implies performance relative to a specified objective over an adequately investigated region. The present matrix supplies several composition-response combinations, but the ranking is not accompanied by a stated objective function or a test of neighboring compositions. TF8 can therefore be prioritized without claiming that its ingredient ratio is uniquely best. Confirmation would need to reproduce the composition and process, demonstrate that the relevant responses persist across batches and determine whether the same ranking remains after gel incorporation. This interpretation uses the observed agreement among endpoints while leaving the untested parts of the design space open.

The composition matrix also limits causal interpretation. TF8 and TF14 shared the listed lipid and drug masses but differed in ethanol and Tween 80, so their response difference cannot isolate either variable. Comparisons elsewhere in the matrix similarly mix composition changes. A claim that increasing a particular ingredient invariably reduced size or increased entrapment would require controlled contrasts or a supported multivariable model. Independent batches would then be needed to establish whether the trend survives manufacturing variation. The present data describe formulation-associated responses rather than a quantified ingredient effect.

ISSN No:-2456-2165 https://doi.org/10.38124/ijisrt/26nov1139

Candidate selection should follow the intended product performance. A small particle size and narrow distribution may help define a reproducible dispersion, but a topical product also requires an appropriate drug state, usable rheology and acceptable local exposure. An unusually high entrapment percentage is not sufficient if the active ingredient cannot leave the carrier or if the apparent association results from incomplete separation. The screened attributes are therefore complementary. Their value depends on the reliability of the underlying measurements and the purpose for which the candidate is selected.

- *Edge Activation and the Limits of Particle Characterization*

Tween 80 was the edge activator documented for this formulation. The lipid-surfactant balance can alter vesicle assembly and drug association, but the direction of those effects must be tested within the actual system. The ibuprofen optimization study used a defined design to examine edge-activator composition; it illustrates a way to separate formulation effects rather than supplying a mechanistic result for the present drug 7.

Film preparation, hydration and gel incorporation may influence different aspects of the final system. Solvent removal defines the material presented for hydration; hydration determines the medium surrounding the newly dispersed components; gel incorporation changes the environment in which those components are tested. A favorable composition ratio does not identify the contribution of any one operation. For example, a change in the apparent size could reflect a different dispersed population, an altered measurement medium or a process difference. These alternatives cannot be resolved from composition alone. A reproducible comparison would therefore hold the process and measurement conditions constant while varying the intended ingredient factor. This is the experimental purpose of controlling the manufacturing history, rather than a claim that a particular undocumented operation caused the reported TF8 response.

The available matrix also changes solvent input together with lipid and surfactant in several comparisons. Ethanol volume is consequently a preparation variable in this record; it is not a measured residual concentration in the finished gel. A claim about ethanol acting within the applied product would require evidence of what remained after evaporation, hydration and incorporation. The same distinction applies to Tween 80: a weighed input establishes nominal composition, while its distribution between vesicles and the surrounding phase was not measured. Treating input quantities and final material states separately avoids assigning a membrane-transport explanation to an ingredient solely because it appears in the preparation table.

The particle measurements should also retain their measurement basis. DLS produces an interpretation of fluctuating scattered light under specified model and medium conditions. Zeta potential is inferred from electrophoretic mobility rather than measured as a direct surface charge. Dilution, conductivity and viscosity inputs therefore matter to how the numerical values are interpreted 11. The selected instrument images preserve information that a summary mean alone would lose, including the distribution shape and acquisition outputs. Their inclusion does not replace the original electronic records needed to verify sample identity and acquisition conditions.

The early transfersome mechanism proposed transport associated with hydration forces and an osmotic gradient 5. That proposal cannot be demonstrated by an egg-membrane release curve or inferred from a PDI below a chosen threshold. A deformation or extrusion experiment, suitable controls and skin localization measurements would be needed to connect the proposed membrane behavior to the prepared carrier. Likewise, intact-vesicle migration and release of dissolved drug are different explanations for tissue delivery. The present record does not discriminate between them. The title and conclusions therefore avoid a claim of verified ultra-deformability or enhanced cutaneous transport.

- *Material Identity and Analytical Interpretation*

The material-form question precedes interpretation of the solubility screen. The source names ruxolitinib but does not establish whether the weighed material was the free base, phosphate salt or another supplied form. The contradictory color descriptions, melting observations and qualitative solubility categories cannot resolve that identity. A certificate of analysis and an appropriate reference comparison would provide a firmer basis. Without them, apparent disagreement with external physical-property descriptions should be investigated rather than repaired by importing a literature value from a different material form.

The solubility procedure also supports a narrower conclusion than its categorical labels suggest. Observing whether 1-2 mg dissolves in 5 mL tests behavior at a low nominal concentration. A fully dissolved sample at that loading supplies a lower bound under the observed conditions, not a saturation concentration. Temperature, pH, equilibration and solid-state changes may influence the result. The complete original solvent list is retained so the experiment is not lost, but those observations should not be used to justify a quantitative sink-condition claim for the diffusion assay.

Calibration agreement is particularly important because several downstream results rely on ultraviolet quantification. Re-fitting the five listed standards produced a slope and intercept different from those printed in the thesis, even though the recalculated R^2 remained close to 0.998. This is a numerical discrepancy rather than evidence that the method necessarily failed. The actual regression input, blank treatment, rounding and original instrument export should resolve it. A revised assay equation must then be applied to the original unknown absorbances and dilution factors; it cannot be used to adjust the reported final percentages by an assumed constant correction.

Q2(R2) provides a framework for analytical validation, including spectroscopic applications 9. Q14 addresses scientific development and control of the analytical procedure

ISSN No:-2456-2165 https://doi.org/10.38124/ijisrt/26nov1139

10. In this study, the relevant practical questions include whether blank gel components interfere, whether extraction is complete and whether the calibration medium represents the analyzed samples. If 100 mg denotes gel mass at the intended 1.5% strength, the described extraction and final dilution would nominally yield 7.5 µg/mL before any recovery loss. This calculation is consistent with the calibration range, but remains conditional on the stated mass basis and confirmed drug strength.

A useful analytical comparison would distinguish blank response, extraction recovery and dilution behavior. A blank gel processed through the same extraction would test whether the vehicle contributes to the measured signal. Addition of a known amount before extraction would examine the combined extraction and measurement process; addition after extraction would examine the response in the extracted matrix. These are proposed diagnostic comparisons, not experiments reported for the current gels. Their purpose would be to locate a bias before correcting final percentages. A low recovery before extraction and an acceptable response after extraction would direct attention toward sample preparation, whereas a changed response in both cases would require examination of matrix effects or calibration conditions.

Filtration introduces another point at which the measured fraction can differ from the initially sampled material. The filter grade was stated, but an assessment of drug loss during filtration was not provided. A comparison of appropriately clarified aliquots with and without the filtration step could address that question, provided that the analytical method and particle-removal procedure were suitable. The same sample basis should then be carried through all calculations. Reporting gel mass, nominal active strength, extraction volume and each dilution factor together would allow a reader to reconstruct the expected concentration before recovery losses. This would make the existing conditional concentration calculation testable rather than converting it into proof that the final gel contained its intended dose.

- *Drug Association and the Dose Carried into the Gel*

The entrapment-method inconsistency changes the meaning of the reported percentage. If free drug is measured in the supernatant, association can be inferred by subtraction from the relevant total. If drug is recovered from the separated sediment, the recovered associated mass belongs in the numerator directly, subject to recovery and carryover controls. The supplied text describes sediment analysis while printing a complement formula with an undefined practical-content term. Neither interpretation can be selected from the final percentage alone. Retaining the value with its provenance is preferable to reverse-engineering a procedure that may never have been used.

The nominal gel strength requires a separate mass balance. A 100 g gel at 1.5% w/w contains 1.5 g drug on the stated basis. The vesicle matrix lists 10 mg per formulation-scale preparation. Before losses, 1.5 g corresponds to 150 such drug-input quantities; this arithmetic does not show that 150 batches were made. It shows that scaling, concentration or a different documented batch size must connect the listed vesicle preparation to the gel. The actual dispersion concentration, recovered quantity, free-drug treatment and incorporated volume would establish that connection. Entrapment efficiency alone cannot supply those missing quantities.

Total drug loading and vesicle association should also be kept as separate balances. A final gel could contain drug recovered with the vesicular fraction, drug remaining in the external phase and drug lost during processing. The entrapment percentage describes an operationally defined fraction only when the separation and assay recoveries are known. It does not establish the concentration of the whole dispersion transferred into the gel. Conversely, a satisfactory whole-gel assay would not demonstrate that the drug remained vesicle-associated. The two measurements are complementary: one concerns the amount present on a defined basis, and the other concerns its distribution under a specified separation procedure. Resolving both balances is necessary before the gel stage can be linked quantitatively to the screened vesicle preparation.

- *Polymer Concentration and Product Handling*

The gel results show a consistent ordering: increasing the listed Carbopol 940 concentration coincided with higher apparent viscosity and lower spreadability and extrudability. A more resistant polymer network is a reasonable formulation-level interpretation, but the single-speed measurement cannot define shear thinning, yield behavior or recovery after application. The magnitude of viscosity also depends on temperature and measurement history. A full rheological profile would be more informative for comparing manufacturing consistency and product handling than a value described simply as optimal.

TG2 occupies an intermediate position in several handling measurements, which explains its role as a compromise candidate. The data do not specify an acceptance interval that makes an intermediate value desirable in every case. TG1 gave faster release and easier spreading in the reported tests, whereas TG3 was more viscous. Selection must relate those differences to a defined product objective. The small differences in reported pH and percentage drug content should also be interpreted descriptively until the replicate structure and assay performance are established. Skin irritation, sensory response and application-site residence were not measured by these tests.

The single-speed viscosity result is most informative when interpreted with the dispensing and spreading tests performed on the same formulation. A high apparent viscosity may coincide with lower extrusion under a particular load, yet the comparison cannot predict behavior at another shear rate or after repeated handling. The present means show an internally consistent ordering across these tests, not a complete description of flow. A more detailed rheological assessment would need to distinguish the response during deformation from recovery afterward and to document temperature and sample history. Such

ISSN No:-2456-2165 https://doi.org/10.38124/ijisrt/26nov1139

measurements would help determine whether TG2's intermediate values are reproducible properties of the gel structure or depend strongly on the test conditions. No yield stress, thixotropic recovery or adhesion value is inferred from the existing data.

➢ *Release Through Egg Membrane and Dermal Delivery*

The release profiles are consistent with an association between higher polymer concentration and slower receptor appearance of drug within the tested apparatus. Gel resistance is one plausible contributor. Drug availability outside vesicles, interaction with the membrane, receptor solubilization and sampling conditions could also contribute. The experiment does not isolate these steps. A nonvesicular ruxolitinib gel, a matched dispersion and a suitable conventional comparator would help distinguish the effect of vesicles from the effect of the semisolid vehicle.

Egg membrane does not reproduce the organized stratum-corneum barrier or drug distribution within viable human skin. OECD Test 428 describes absorption testing with human or animal skin and assessment of drug distribution in the test system 13. Consequently, the present percentage recovered in a receptor compartment should be described as a diffusion or release endpoint under the stated membrane conditions. Calling it cumulative skin flux would change both the biological model and the quantity measured. A flux requires a verified recovered amount, area and appropriate time-dependent analysis, which the supplied percentages do not provide.

The FDA IVRT document cited here is a 2022 draft intended for comparative studies supporting generic topical-product bioequivalence 12. It provides relevant testing context, but does not certify this academic egg-membrane method as validated or make its recommendations an acceptance specification for a new gel. The missing dose, sampling volume and sink-condition evidence limit reconstruction of the assay. An appropriate next comparison would control applied dose and receptor conditions and separately measure release, skin retention and receptor recovery. Each endpoint would then answer a defined part of the delivery question.

A comparison designed to distinguish carrier and vehicle effects would retain the same applied active amount while changing one component of the system at a time. A nonvesicular drug gel could test whether the observed profile requires the vesicular preparation. A dispersion assessed before gel incorporation could help separate the effect of the polymeric vehicle from that of the dispersion, although differences in donor geometry would still need control. A membrane-only recovery check would identify whether the barrier or receptor conditions contribute to an apparent loss. These controls are proposed ways to investigate the current interpretation; their outcomes cannot be predicted from the three gel curves.

Mass recovery would connect those comparisons to the physical meaning of the release percentage. Drug remaining in the donor, associated with the membrane and recovered in the receptor should be quantified on compatible bases. If receptor recovery decreased while donor recovery increased, the result would support a different interpretation from a simultaneous reduction in all measured compartments. In the latter case, incomplete extraction, adsorption or degradation would need investigation. The present record does not contain these compartment measurements. The proposed comparison therefore defines how a future experiment could distinguish slower transfer from incomplete recovery without claiming that either explanation has already been established for TG3.

➢ *Interpreting the Kinetic Fits*

Reproduction of the full-profile regressions is useful because it confirms that the plotted model statistics are largely consistent with the TG2 means. This check remains mathematical. It does not authenticate the underlying observations or show that a particular transport model governs the formulation. The first-order, Higuchi and power-law regressions had similar high coefficients of determination, but were fitted in different transformed response spaces. Ranking them by R^2 alone obscures that difference and the assumptions behind each transformation.

The free-intercept zero-order fit predicts nonzero release at time zero and values above 100% near the end of the interval. The free-intercept square-root fit also has a negative intercept and exceeds 100% at its fitted 12-hour value. These features identify the fits as descriptive approximations over the supplied data, with limited extrapolative meaning. The original intercepts were preserved for comparison rather than silently forced to physically convenient values. Changing constraints would constitute a different model fit and should be reported as such.

The full-profile power-law slope of approximately 0.6573 differed from the early-profile slope of approximately 0.7335. The difference demonstrates sensitivity to the chosen fitting interval. The power-law literature concerns particular matrix geometries and stages of release, so an exponent from a vesicle-containing gel behind a second membrane should not automatically be assigned a universal mechanistic label 14,15. Likewise, a good square-root relation does not prove that all assumptions of the Higuchi derivation hold 16. Replicate profiles and a justified model domain would support a more informative kinetic analysis.

Response transformation also changes how deviations contribute to a fitted line. For the first-order plot, the logarithm is applied to the percentage remaining. As release approaches completion, a fixed absolute change in the remaining percentage produces a larger change in its logarithm than it does earlier in the profile. The late observations can therefore have a different influence on the transformed fit from their influence on a fit to untransformed release. This is a mathematical property of the transformation, not evidence of a change in the experiment. It explains why agreement of transformed R^2 values should be considered alongside the response definition, residual pattern and intended fitting domain rather than treated as a direct comparison of transport mechanisms.

ISSN No:-2456-2165 https://doi.org/10.38124/ijisrt/26nov1139

The interpolation and regression summaries also answer different questions. Interpolation reports where a chosen segment of the observed mean curve crosses a threshold; regression describes agreement with a selected functional relationship over an interval. A curve can have a later interpolated threshold time without being governed by a different release mechanism. Likewise, the very high early-profile power-law R^2 applies to five transformed mean points and does not quantify between-batch reproducibility. The current summaries are therefore presented as complementary numerical descriptions. Their interpretation would be strengthened by replicate profiles analyzed on the same sampling schedule and by an a priori decision about which part of the profile the model is intended to describe.

- *Relationship to Established Ruxolitinib Formulations*

The clinical cream trials establish that ruxolitinib can produce indication-specific benefit when delivered in an appropriate conventional vehicle 2,3. They do not show that this transfersomal gel improves local exposure, safety or patient outcomes. Comparisons with cream pharmacokinetics must likewise preserve the original application conditions and formulation 4. The relevant development question is therefore an incremental formulation benefit measured against a matched comparator, rather than a general statement that a nanocarrier is required for the molecule to work topically.

The published ruxolitinib nanoliposomal formulation provides a drug-specific comparison of research approaches 8. Its carrier, composition and testing conditions differ from the present system. Numerical particle or entrapment values across those studies should not be interpreted as a competition with a common assay basis. Transfersomal gel experiments with asiatic acid similarly demonstrate a strategy for linking formulation and delivery measurements, while remaining indirect evidence for ruxolitinib 6. The present work would contribute most clearly through reproducible composition, transparent analytical methods and a direct test of the intended delivery advantage.

A formulation comparison would be clearest if active strength, application amount, test area and sampling conditions were reconciled before interpreting the carrier effect. Equal nominal strength alone does not ensure equal applied drug mass when donor amounts differ. Equal applied mass also does not make dissimilar barrier models interchangeable. A comparison with an established cream would consequently need a defined experimental question, such as receptor appearance or distribution within skin, together with a method suited to that endpoint. Published cream pharmacokinetics demonstrate the importance of cream strength and application conditions for exposure 4; they do not provide a numerical correction that can be applied to an egg-membrane gel experiment. This limits the scope of a cross-study comparison while preserving its value for designing a direct test.

- *Storage Findings and Remaining Experimental Limitations*

The three-week storage series retained gross appearance and showed small reported decreases in drug content. Those observations are compatible with short-term maintenance of the tested attributes, conditional on confirmation of the source data. They do not establish that the vesicles retained their original size, associated-drug fraction or release behavior. A visually homogeneous gel can still undergo changes that are not apparent by inspection. The absence of replicated storage values and a demonstrated stability-indicating assay also prevents a confident interpretation of the small numerical differences between conditions.

Q1A(R2) treats stability evidence as the basis for evaluating change with time and supporting a justified storage period 17. The supplied study was much narrower than a registration stability program and should be described accordingly. A defensible continuation would define the final container, storage conditions and sampling plan, then examine assay, relevant degradation, particle properties and product performance. The current record supplies an initial set of observations rather than a shelf-life claim.

The meaning of a small assay decrease depends on whether the method distinguishes intact drug from other responses in the stored sample. Without that distinction, a content change cannot be assigned solely to chemical degradation. Changes in extraction, dispersion homogeneity or sample handling could also affect the measured percentage. A future storage comparison would therefore need an assay suited to the stability question and sampling that represents the container contents. Measurements of particle properties and release would address physical or performance changes that an assay value alone may miss. These are separate observations: an unchanged appearance does not establish unchanged vesicle properties, and a small assay change does not by itself identify the pathway responsible.

The largest limitation is the unresolved experimental provenance of datasets labeled illustrative in the source. That issue precedes statistical refinement. It can be addressed by linking each formulation code to manufacturing records, sample identifiers, instrument exports and individual assay calculations. The remaining limitations concern material identity, incomplete process settings, the entrapment numerator, assay calibration, gel dose reconciliation and a diffusion model that does not measure cutaneous delivery. The manuscript retains every supplied experimental dataset so these questions can be resolved against the full record. Until then, TF8 and TG2 remain candidates for confirmation rather than validated formulations ready for clinical interpretation.

V. CONCLUSION

The thesis-reported formulation series describes ruxolitinib transfersomes prepared from soya phosphatidylcholine, Tween 80 and ethanol, followed by incorporation into Carbopol 940 gels. TF8 combined the most

ISSN No:-2456-2165 https://doi.org/10.38124/ijisrt/26nov1139

favorable reported particle profile with the highest reported entrapment, while TG2 provided intermediate handling properties and 96.18 ± 0.54% reported release at 12 hours through egg membrane. The complete formulation, characterization, release, transformation and storage data have been retained. Recalculation supported the principal release-model statistics but identified a calibration-equation discrepancy and a fitting-range effect on the power-law exponent.

These findings define a candidate-development pathway rather than demonstrate enhanced dermal transport. Several numerical series were labeled illustrative in the source, and their experimental provenance remains unresolved. Confirmation requires primary laboratory records, a reconciled drug-association assay, verified gel drug loading and adequately described manufacturing conditions. Skin-specific deposition and permeation measurements, suitable comparators, local tolerability and longer storage assessment would then determine whether the candidate has a delivery advantage. No claim of therapeutic superiority, reduced systemic exposure or established shelf life is supported by the present record.

➢ *Data Availability*

The source-reported numerical datasets, experimental images and recalculated transformation results are included in this manuscript. Individual replicate readings, original instrument files and batch-manufacturing records were not available for independent verification. No public-repository accession or newly generated laboratory dataset is claimed.

REFERENCES

[1.] Smith P, Yao W, Shepard S, Covington M, Lee J, Lofland J, et al. Developing a JAK inhibitor for targeted local delivery: ruxolitinib cream. Pharmaceutics. 2021;13(7):1044. doi: 10.3390/pharmaceutics13071044.

[2.] Papp K, Szepietowski JC, Kircik L, Toth D, Eichenfield LF, Leung DYM, et al. Efficacy and safety of ruxolitinib cream for the treatment of atopic dermatitis: results from 2 phase 3, randomized, double-blind studies. J Am Acad Dermatol. 2021;85(4):863-872. doi: 10.1016/j.jaad.2021.04.085.

[3.] Rosmarin D, Passeron T, Pandya AG, Grimes P, Harris JE, Desai SR, et al. Two phase 3, randomized, controlled trials of ruxolitinib cream for vitiligo. N Engl J Med. 2022;387(16):1445-1455. doi: 10.1056/NEJMoa2118828.

[4.] Gong X, Chen X, Kuligowski ME, Liu X, Liu X, Cimino E, et al. Pharmacokinetics of ruxolitinib in patients with atopic dermatitis treated with ruxolitinib cream: data from phase II and III studies. Am J Clin Dermatol. 2021;22(4):555-566. doi: 10.1007/s40257-021-00610-x.

[5.] Cevc G, Blume G. Lipid vesicles penetrate into intact skin owing to the transdermal osmotic gradients and hydration force. Biochim Biophys Acta. 1992;1104(1):226-232. doi: 10.1016/0005-2736(92)90154-E.

[6.] Opatha SAT, Titapiwatanakun V, Boonpisutiinant K, Chutoprapat R. Preparation, characterization and permeation study of topical gel loaded with transfersomes containing asiatic acid. Molecules. 2022;27(15):4865. doi: 10.3390/molecules27154865.

[7.] Vieira J, Castelo J, Martins M, Saraiva N, Rosado C, Pereira-Leite C. Mixed edge activators in ibuprofen-loaded transfersomes: an innovative optimization strategy using Box-Behnken factorial design. Pharmaceutics. 2023;15(4):1209. doi: 10.3390/pharmaceutics15041209.

[8.] Naeimifar A, Ahmad Nasrollahi S, Akbari Javar H, Nassiri Kashani M, Firooz A, Rouini M. Designing a topical nanoliposomal formulation of ruxolitinib phosphate. Pharm Sci. 2023;29(1):75-83. doi: 10.34172/PS.2022.17.

[9.] US Food and Drug Administration. Q2(R2) validation of analytical procedures. Guidance for industry. March 2024. Available online.

[10.] US Food and Drug Administration. Q14 analytical procedure development. Guidance for industry. March 2024. Available online.

[11.] Bhattacharjee S. DLS and zeta potential - what they are and what they are not? J Control Release. 2016;235:337-351. doi: 10.1016/j.jconrel.2016.06.017.

[12.] US Food and Drug Administration. In vitro release test studies for topical drug products submitted in ANDAs. Draft guidance for industry. October 2022. Available online.

[13.] Organisation for Economic Co-operation and Development. Test No. 428: skin absorption: in vitro method. OECD Guidelines for the Testing of Chemicals, Section 4. Paris: OECD Publishing; 2004. doi: 10.1787/9789264071087-en.

[14.] Korsmeyer RW, Gurny R, Doelker E, Buri P, Peppas NA. Mechanisms of solute release from porous hydrophilic polymers. Int J Pharm. 1983;15(1):25-35. doi: 10.1016/0378-5173(83)90064-9.

[15.] Ritger PL, Peppas NA. A simple equation for description of solute release II. Fickian and anomalous release from swellable devices. J Control Release. 1987;5(1):37-42. doi: 10.1016/0168-3659(87)90035-6.

[16.] Siepmann J, Peppas NA. Higuchi equation: derivation, applications, use and misuse. Int J Pharm. 2011;418(1):6-12. doi: 10.1016/j.ijpharm.2011.03.051.

[17.] International Council for Harmonisation. Q1A(R2) stability testing of new drug substances and products. Step 4 guideline. 6 February 2003. Available online.